OMH2O README FILE

This document was created on 10 May 2019 for Version 4 OMI total column water vapor product.

Overview

This document provides a brief description of the OMH2O product for this data release (Version 4). OMH2O contains Total Column Water Vapor (TCWV) and ancillary information retrieved from OMI measurements using SAO's v4.0 retrieval algorithm. This algorithm uses nonlinear least-squares fitting for the OMI visible spectra to derive slant column density (SCD) and uses Air Mass Factor (AMF) to convert slant column density to vertical column density. 10^{23} molecules/cm^2 = 29.89 mm of TCWV. In global mode, each file contains a single orbit of data covering a swath approximately 2,600 km wide from pole to pole (sunlit portions only).

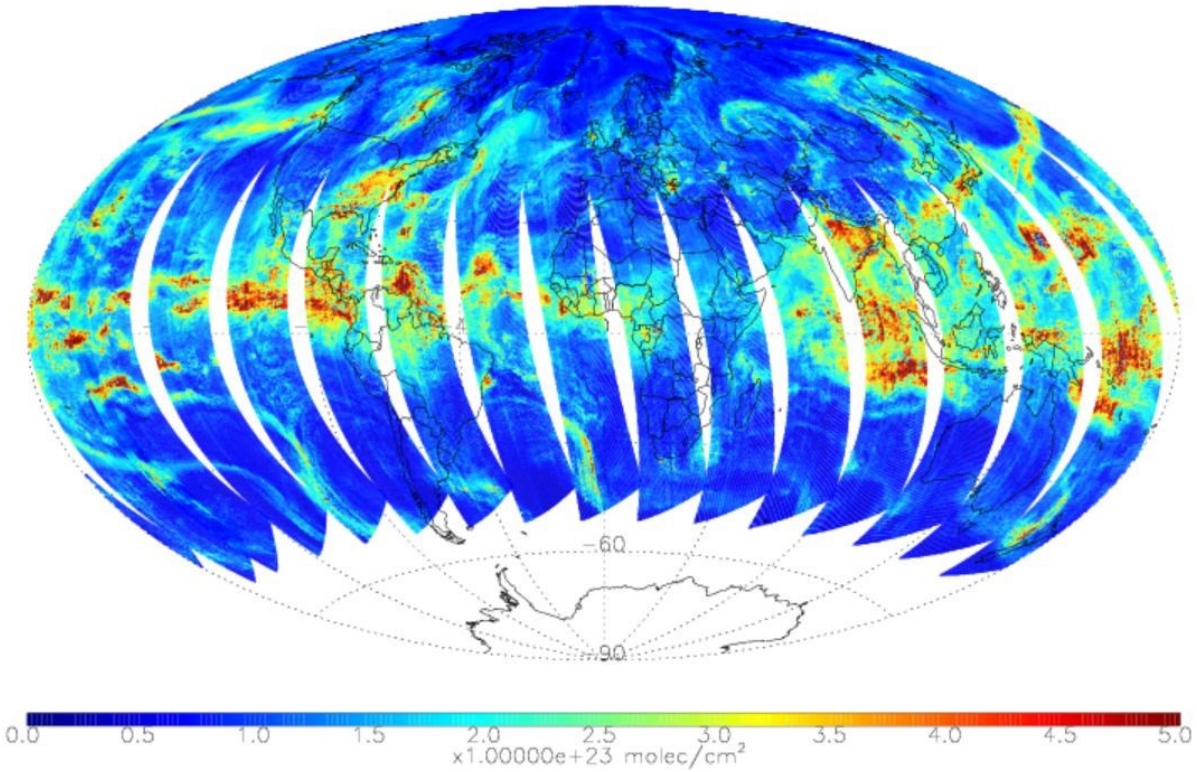

The image above shows the water vapor vertical column for 14 July 2005.

Release History

OMH2O Algorithm Version[1]	4.0
Collection/Product Version	003
This Public Release	May 2019
First Public Release	20 August 2014
Known Issues	Row anomaly, stripes, occasional outliers

[1]Algorithm version (Level-2 related) and Collection/Product version are different. The collection/product version number is part of any OMH2O data file name, e.g., OMI-Aura-L2-OMH2O_<acquisition date>-o<orbit number>_v003-<processing date>.he5, and refers to the OMI L1B data collection used in the retrieval.

Algorithm Description

Slant column is derived through direct spectral fitting of radiances and irradiances. The main steps are (1) Radiance wavelength calibration, which finds the optimum wavelength registration for each swath [Chance and Kurucz, 2010]. This determines a common wavelength grid for auxiliary data bases, such as the reference spectra; (2) Non-linear least-squares fitting for each OMI spectrum.

Water vapor slant column fitting uses the spectral window of 432.0 – 465.5nm which is measured by the visible channel of OMI. In addition to the target molecule H_2O, the following interference molecules are included in the fitting – ozone, NO_2, liquid water, O_2-O_2 collision complex, $C_2H_2O_2$ and IO. The inelastic Raman scattering or Ring effect, water Ring effect, vibrational Raman scattering of air and under-sampling are also considered. Third order additive and multiplicative closure polynomials are employed in the fitting.

Water vapor slant columns are converted to vertical columns using the AMFs calculated with the help of a look-up table. The table is pre-computed using a radiative transfer model (VLIDORT [Spurr, 2006]). Variables in the look-up table include surface albedo, surface pressure, cloud fraction, cloud pressure, solar zenith angle, viewing zenith angle and relative azimuth angle. The scattering weight of each retrieval is interpolated from the look-up table using the parameter values of the scene. Cloud fraction and cloud top pressure are from the OMCLDO2 product [Veefkind et al., 2016]. Surface albedo is from the OMLER database [Kleipool et al., 2008]. The monthly mean 2 PM H_2O vertical profiles derived from the GEOS-5 MERRA2 data assimilation product is used to convolve with the scattering weight in AMF calculation.

Cross-track striping is a common problem for OMI product. It is due to instrumental systematic error. The vertical columns provided with this release are not de-striped. The user can choose to post-process them with his / her own program. One de-striping method is to (1) recover the slant column using the product of the vertical column and AMF, (2) derive a cross-track correction vector based on the normalized average of multiple lines and swaths (3) apply the correction vector to slant column (4) divide slant column by AMF to get vertical column.

More details on the 2-step retrieval algorithm can be found in the OMI Algorithm Theroretical Basis Document (ATBD) Vol. 4. A summary of the OMI water vapor algorithm can be found in Table 2.

Data Quality Assessment

Vertical columns in this release have not been de-striped.

Pixels affected by row anomaly have been flagged in the Geolocation field XtrackQualityFlags and XtrackQualityFlagsExpanded. We recommend not using data affected by row anomaly.

FittingRMS and ColumnUncertainty are provided with the retrieval. Since clouds lead to large uncertainties, best data should have little cloud contamination. User can select data according to cloud fraction threshold along with other criteria, for example, cloud fraction<0.05, cloud top pressure > 750 hPa, Fitting RMS<0.001, MDQFL = 0, etc.

Cloud Information

The OMH2O product contains two data fields about clouds – AMFCloudFraction and AMFCloudPressure. These are based on the OMCLDO2 cloud product and provided here for cloud filtering purpose. They are not

identical to those in OMCLDO2 and should not be used for independent cloud studies. These fields are modified from OMCLDO2 for AMF calculation as in [Gonzalez Abad et al., 2016]. In addition, the ice/snow flag in the OMCLDO2 product was used to further correct the values.

Validation

Validation of this data release was performed for 2006 by comparisons with GPS network data over land and SSMIS data over the oceans. Results and recommendations for data filtering criteria can be found in Wang et al. [2019]. This version generally compares better with the reference datasets than Version 3 which has much larger positive bias.

Data Quality Flag

Similar to other SAO standard data products (BrO, HCHO, OClO), the H_2O product contains the MainDataQualityFlag. It can be used to filter the data.

Value	**Classification**	**Rationale**
0	Good	Column value present and passes all quality checks; data may be used when properly filtered along with other criteria.
1	Suspicious	Caution advised because one or more of the following conditions are present: • *FitConvergenceFlag* is < 300 (but > 0): convergence at noise level • Column+2σ uncertainty < 0 (but Column+3σ uncertainty ≥ 0) • Absolute column value > *MaximumColumnAmount* ($5 \cdot 10^{23}$ molecules/cm^2)
2	Bad	Avoid using data because one or more of the following conditions are present: • *FitConvergenceFlag* is < 0: abnormal termination, no convergence • Column+3σ uncertainty < 0
≤ -1	Missing	No column values are computed; entries are missing

Additional information

The OMH2O product is in HDF-EOS5 format. A single file contains information retrieved from each pixel of an OMI granule. The files include vertical column density, AMF, scattering weight, surface pressure, a priori water vapor profile, slant column fitting uncertainty, geolocation, geometry, data quality flag and other ancillary information. The scattering weights can be used with other water vapor profiles to derive AMF as needed to get more accurate estimates of vertical column density.

For questions and comments about the OMH2O dataset, please contact Huiqun Wang (hwang@cfa.harvard.edu) and cc Kelly Chance (kchance@cfa.harvard.edu) who has the overall responsibility for this product.

Summary of algorithm fitting specifics

Fitting window	432.0-466.5 nm
Baseline polynomial	3rd order
Scaling polynomial	3rd order
Instrument slit function	Hyper-parameterization of pre-flight slit function [Dirksen et al., 2006]
Solar reference spectrum	Dobber et al. [2008]
H_2O cross section	280K, HITRAN 2008 [Rothman et al., 2009]]
O_3 cross section	228K, Brion et al. [1993]
NO_2 cross section	220K, Vandaele et al. [1998]
Liquid water	Mason et al. [2016]
O_2-O_2 cross section	293K, Thalman and Volkamer [2013]
$C_2H_2O_2$ cross section	296K, Volkamer et al. [2005]
IO	298K, Spietz et al. [2005]
Molecular Ring	Chance and Spurr [1997]
Water Ring	Chance and Spurr [1997]
Undersampling	On-line computation [Chance et al., 2005]
Air Vibrational Raman	Lampel et al. [2015]

Selected List of Elements in an OMH2O Output File

The tables below show a selected list of data elements in an OMH_2O HDF-EOS5 output file. The tables are divided into (*a) Swath Dimensions*, *(b) Geolocation Fields*, and *(c) Data Fields*. For a complete list of fields, please refer to OMSAO_FileSpecifications_README.pdf.

(a) Swath Dimensions

Field Name	Field Type	Description
nTimes	HE5T_NATIVE_INT	Number of swath lines in an OMI granule (usually about 1650)
nXtrack	HE5T_NATIVE_INT	Number of cross-track positions in a swath line (usually 30 or 60)
nUTCdim	HE5T_NATIVE_INT	Number of elements in a single *TimeUTC* field entry (6)
Nlevels	HE5T_NATIVE_INT	Number of GEOS-Chem climatology levels

(b) Geolocation Fields of prime interest

Field Name	Field Type	Dimensions	Description
Latitude	HE5T_NATIVE_FLOAT	nXtrack,nTimes	Geodetic latitude [deg] at the center of the ground pixel
Longitude	HE5T_NATIVE_FLOAT	nXtrack,nTimes	Geodetic longitude [deg] at the center of the ground pixel
SolarZenithAngle	HE5T_NATIVE_FLOAT	nXtrack,nTimes	The solar zenith angle [deg] at the center of the ground pixel
TimeUTC	HE5T_NATIVE_INT16	nUTCdim,nTimes	UTC value of the TAI93 time. The 6 different elements of the UTC string YYYY-MM-DD hh:mm are stored in the 6 arrays positions.
ViewingZenithAngle	HE5T_NATIVE_FLOAT	nXtrack,nTimes	The viewing zenith angle [deg] at the center of the ground pixel
XtrackQualityFlags	HE5T_NATIVE_INT8	nXtrack,nTimes	Cross-Track quality flags as set in the L1b to flag row anomaly
XtrackQualityFlagsExpanded	HE5T_NATIVE_INT16	nXtrack,nTimes	Cross-Track quality flags as set in the L1b to flag row anomaly. Expanded human-readable version of XtrackQualityFlags

(c) Data Fields of prime interest

Field Name	Field Type	Dimensions	Description
AirMassFactor	HE5T_NATIVE_DOUBLE	nXtrack,nTimes	Molecule specific air mass factor for each ground pixel
AMFCloudFraction	HE5T_NATIVE_FLOAT	nXtrack,nTimes	Adjusted Cloud fraction
AMFCloudPressure	HE5T_NATIVE_FLOAT	nXtrack,nTimes	Adjusted Cloud pressure
Albedo	HE5T_NATIVE_DOUBLE	nXtrack,nTimes	Ground pixel albedo from the OMLER database for the central wavelength of the fitting window
ColumnAmount	HE5T_NATIVE_DOUBLE	nXtrack,nTimes	Total vertical column amount [mol/cm^2] for each ground pixel
ColumnUncertainty	HE5T_NATIVE_DOUBLE	nXtrack,nTimes	Total slant column amount uncertainty [mol/cm^2] for each ground pixel
GasProfile	HE5T_NATIVE_DOUBLE	nXtrack,nTimes, nLevels	Vertical profiles used in the AMFs calculation
MainDataQualityFlag	HE5T_NATIVE_INT16	nXtrack,nTimes	Main flag to indicate data quality (see above)
PixelCornerLatitudes	HE5T_NATIVE_FLOAT	nXtrack+1,nTimes+1	The geodetic latitudes [deg] of the corner coordinates of the OMI ground pixels.
PixelCornerLongitudes	HE5T_NATIVE_FLOAT	nXtrack+1,nTimes+1	The geodetic longitudes [deg] of the corner coordinates of the OMI ground pixels.
ScatteringWeights	HE5T_NATIVE_DOUBLE	nXtrack,nTimes, nLevels	Scattering weights used n the AMFs calculation

References

OMI Algorithm Theoretical Basis Document, Volume IV, OMI Trace Gas Algorithms, OMI-ATBD-VOL4, ATBD-OMI-04, Version 2.0, August 2002.

Brion, J., A., Chakir, D., Daumont, J., Malicet, and C., Parisse, 1993. High-resolution laboratory absorption cross-section of O2 – temperature effect, Chem. Phys. Lett., 213, 610-612, doi:10.1016/0009-2614(93)89169-I.

Chance, K, and R.J.D. Spurr, 1997. "Ring effect studies: Rayleigh scattering, including molecular parameters for rotational Raman scattering, and the Fraunhofer spectrum", *Applied Optics*, 36, 5224-5230.

Chance, K., T.P. Kurosu, and C.E. Sioris, 2005. Undersampling correction for array-detector based satellite spectrometers, Applied Optics 44(7), 1296-1304.

Chance, K. and Kurucz, R., 2010. An improved high-resolution solar reference spectrum for earth's atmosphere measurements in the ultraviolet, visible, and near infrared, J. Quant. Spectrosc. Ra., 111, 1289–1295, doi:10.1016/j.jqsrt.2010.01.036.

Dirksen, R., Dobber, M., Voors, R., and Levelt, P., 2006. Prelaunch characterization of the Ozone Monitoring Instrument transfer function in the spectral domain, Appl. Optics, 45, 3972–3981, doi:10.1364/AO.45.003972.

Dobber, M., Voors, R., Dirksen, R., Kleipool, Q. and Levelt, P., 2008. The high-resolution solar reference spectrum between 250 and 550 nm and its application to measurements with the Ozone Monitoring Instrument, Solar Physics, 249, 2, 281-291, doi:10.1007/s11207-008-9187-7.

Kleipool, Q. L., M. R. Dobber, J. F. De Haan, and P. F. Levelt, 2008. "Earth surface reflectance climatology from three years of OMI data", J, Geophys. Res., 113, D18303, doi:10.1029/2008JD010290.

Lampel, J., Frieß, and Platt, U., 2015. The impact of vibrational Raman scattering of air on DOAS measurements of atmospheric trace gases, Atmos. Meas. Tech., 8, 3767-3787, doi:10.5194/amt-8-3767-2015.

Mason, J.D., Cone, M.T., and Fry, E.S., 2016. Ultraviolet (250-550 nm) absorption spectrum of pure water. Applied Optice, 55, 25, 7163-7172, doi:10.1364/AO.55.007163.

Rothman, L. S., Gordon, I. E., Barbe, A., et al., 2009. The HITRAN 2008 molecular spectroscopic database, J. Quant. Spectrosc. Radiat. Transfer, 110, 533–572, 2009.

Spietz, P., Martin, J. C. G. and Burrows, J. P., 2005. Spectroscopic studies of the I-2/O-3 photochemistry – Part 2. Improved spectra of iodine oxides and analysis of the IO absorption spectrum, J. Photochemistry and Photobiology, 176 (1-3), 50-67, doi:10.1016/j.photochem.2005.08.023.

Spurr, R.J.D., 2006. "VLIDORT: a linearized pseudo-spherical vector discrete ordinate radiative transfer code for forward model and retrieval studies in multilayer multiple scattering media", J. Quant. Spectr. Radiat. Tran., 102, 316-342, doi:10.1016/j.jqsrt.2006.05.005.2006.

Thalman, R. and Volkamer, R., 2013. Temperature dependent absorption cross-sections of O2-O2 collision pairs between 340 and 630 nm and at atmospherically relevant pressure, Phys. Chem. Chem. Phys., 15, 15371-15381, doi:10.1039/c3cp50968k.

Vandaele A.C., C. Hermans, P.C. Simon, M. Carleer, R. Colin, S. Fally, M.F. Mérienne, A. Jenouvrier, and B. Coquart, 1998. Measurements of the NO_2 absorption cross-section from 42000 cm^{-1} to 10000 cm^{-1} (238-1000 nm) at 220 K and 294 K, Journal of Quantitative Spectroscopy and Radiative Transfer, 59, pp 171-184.

Volkamer, R., P., Spietz, J., Burrows, and U., Platt, 2005. High-resolution absorption cross-section of glyoxal in the UV/vis and IR spectral ranges, J. Photochem. Photobio., 172, 35-46, doi:10.1016/j.jphotochem.2004.11.011.

Veefkind, J.P., de Hann, J.F., Sneep, M., and Levelt, P.F., 2016. Improvements to the OMI O2-O2 operational cloud algorithm and comparisons with ground-based radar-lidar observations. Atmos. Meas. Tech., 9, 6035-6049, doi:10.5194/amt-9-6-35-2016.

Wang, H. Souri, A. H., Gonzalez Abad, G., Liu, X. and Chance, K., 2019. OMI total column water vapor Version 4 Validation and Applications, Atmos. Meas. Tech. Discuss., https://doi.org/10.5194/amt-2019-89.